ISSN (Online) 2287-3406
Journal of Life Science **2024** Vol. 34. No. 7. 443~452 DOI : https://doi.org/10.5352/JLS.2024.34.7.443

L-AHG-mediated Suppression of M1 Polarization and Pro-inflammatory Signaling Pathways in LPS-stimulated RAW264.7 Macrophages

Won Young Jang[1], Shin Young Park[1,2], Ki Youn Kim[1,2], Do Youn Jun[2], Young-Seuk Bae[1,2] and Young Ho Kim[1,2*]

[1]*Laboratory of Immunobiology, School of Life Science and Biotechnology, College of Natural Sciences, Kyungpook National University, Daegu 41566, Korea*
[2]*AT-31 BIO Inc., 403 Business Incubation Center, Kyungpook National University, 80 Daehak-ro, Buk-gu, Daegu 41566, Korea*

Received June 29, 2024 /Accepted July 4, 2024

This study aimed to examine the influence of 3,6-anhydroxygalactose (L-AHG) on the pro-inflammatory M1 polarization and pro-inflammatory responses observed in the RAW264.7 mouse macrophage cell line following stimulation with lipopolysaccharides (LPS). L-AHG exhibited a significant and dose-dependent inhibition of inducible nitric oxide synthase (iNOS) expression, a hallmark of M1 polarization, and subsequent NO production in LPS-stimulated RAW264.7 cells. Furthermore, the LPS-induced upregulation of cyclooxygenase-2 (COX-2), which drives the production of prostaglandin E2, an inflammatory mediator, was also inhibited by L-AHG. L-AHG did not affect the LPS-triggered Toll-like receptor 4 (TLR4)-mediated pro-inflammatory signaling pathway, which culminated in the activation of transforming growth factor-β-activated kinase 1 (TAK1). However, it was observed to inhibit the generation of reactive oxugen species (ROS) in a dose-dependent manner, as well as the TAK1-driven activation of JNK and p38 MAPK. Given that the active p38 MAPK is known to contribute to the assembly of active nicotinamide adenine dinucleotide phosphate (NADPH) oxidase, which catalyzes the intracellular generation of pro-inflammatory ROS in LPS-stimulated macrophages, the dose-dependent reduction in the LPS-induced ROS generation by L-AHG may be mainly due to the prevention of TAK1-driven activation of p38 MAPK. Together, these results demonstrate that the L-AHG-mediated inhibition of the TAK1-JNK/p38 MAPK activation phase of the pro-inflammatory signaling pathway in LPS-stimulated RAW264.7 cells by L-AHG represents a promising mechanism for suppressing M1 polarization and pro-inflammatory responses in macrophages.

Key words : 3,6-Anhydro-L-galactose, anti-inflammatory efficacy, LPS-induced inflammation, M1 polarization, suppressing TAK1-JNK/p38MAPK pathway

Introduction

Macrophages are versatile immune cells originating from embryogenesis or monocyte differentiation. Macrophages can adopt a variety of phenotypes based on their origin and tissue environment, which allows them to respond to different stimuli and microenvironments [3]. Three principal macrophage phenotypes (M0, M1, and M2) are present within human tissues. Naive (M0) macrophages recognize pathogens and are capable of phagocytosis. Upon stimulation by specific signals, M0 macrophages can reversibly polarize into either M1 or M2 macrophages [29]. The M1 type is characterized by its pro-inflammatory properties. These cells secret pro-inflammatory cytokines (IL-1, IL-6, and TNF-α) as well as nitric oxide (NO), which facilitates the effective killing of pathogens [3]. M1 polarization can be induced by Gram-negative bacterial cell wall lipopolysaccharide (LPS) and cytokines (IFN-γ and TNF-α), which activate the transcription factor NF-kB/AP-1 and the expression of inducible nitric oxide synthase (iNOS) [27, 36]. On the other hand, the M2 type exhibits anti-inflammatory properties. They are distinguished by their high phagocytic capacity, the production of extracellular matrix components, and cytokine IL-10 and arginase-1 [4]. M2 polarization is induced by several factors, including fungal cells, parasites, immune complexes, apoptotic cells, Th2 cytokines (IL-4, IL-10, and IL-13), and tumor

***Corresponding author**
Tel : +82-53-218-3111, Fax : +82-53-218-3112
E-mail : ykim@knu.ac.kr

growth factor-beta (TGF-β) [31]. M2 macrophages play a role in the resolution of inflammation, the clearance of apoptotic cells, and the promotion of wound healing and tissue repair.

The balance between M1 and M2 polarization is critical for maintaining of homeostasis within the body, as their dysregulation can significantly impact disease processes [11, 22, 25]. In chronic kidney disease (CKD), M1 macrophages have been demonstrated to contribute to renal injury, suggesting that macrophage polarization may prove an effective strategy for alleviating the disease. In osteoarthritis (OA), the role of the NF-κB pathway in M1 polarization underscores the potential therapeutic value of targeting Toll- like receptors (TLRs) [38]. The reprogramming of macrophages from M1 to M2 and vice versa is currently being investigated as a potential therapeutic strategy [5, 26].

The LPS-induced response of macrophages *in vivo* is of great importance in the context of inflammation, sepsis, and autoimmune diseases [6]. This response results in the excessive production of pro-inflammatory mediators due to macrophage polarization toward the M1 type [20, 35]. This process is initiated by Toll-like receptor 4 (TLR4) signaling, which is activated by LPS, and involves both MyD88- and TRIF-dependent pathways [9]. Several studies highlight the importance of the Toll/IL-1 receptor (TIR) domain in initiating signaling after TLR4 is stimulated by LPS. The TIR domain recruits adaptors like MyD88, TIRAP (MAL), TRAM, and TRIF. In the MyD88-dependent pathway, LPS-stimulated TLR4 recruits MyD88 and TIRAP, which recruit IRAK4 and IRAK1. IRAK4 phosphorylates IRAK1, leading to interaction with TRAF6 and the forming a complex with TAK1 and TAB2. This complex translocates to the cytosol, where TRAF6 is auto-ubiquitinated, leading to TAK1 activation and subsequent activation of IKK and mitogen-activated protein kinases (MAPKs) such as ERK, JNK, and p38 MAPK [9, 24, 30]. This cascade activates NF-κB and AP-1, promoting transcription of inflammatory genes such as COX-2, TNF-α, IL-1β, and IL-6. In the TRIF-dependent pathway, TLR4 recruits TRIF and TRAM, which activate NF-κB and IRF3, leading to the production of Type 1 interferons (IFN-α and IFN-β). These interferons activate STAT1, inducing the transcription of iNOS [9, 10, 24]. Furthermore, reactive oxygen species (ROS) have been demonstrated to play a role in enhancing NF-κB activation [14, 19]. The elevation of intracellular ROS levels in LPS-treated macrophages is a consequence of the assembly of active NADPH oxidase from the subunits, which is initiated following p38 MAPK-mediated phosphorylation of the p47phox subunit [19, 21]. A better understanding of the molecular and cellular mechanisms involved in the activation and polarization of macrophages is a prerequisite for the development of new therapeutic strategies to modulate macrophages functions in pathological situations.

Agar is a food substance consumed for a considerable length of time and registered as a healthy, functional food by the U.S. Food and Drug Administration (FDA, PB265502, GRAS). The Expert Committee on Additives-JECFA also classifies healthy foods as A1, which are not limited food with an acceptable daily intake. Agar is a complex polysaccharide that constitutes the cell wall of marine red algae. It is composed of two major components, agarose and agaropectin [1]. Agarose is a non-ionic linear polymer consisting of a repeating unit of the disaccharide neoagarobiose (NA2), in which 3,6-anhydro-L-galactose (L-AHG) is connected to β-D-galactose (D-Gal) by an α-1,3-linkage, and the resulting NA2 is linked by a β-1,4-glycosidic bond between D-Gal and L-AHG [8].

With regard to the bioactivities of L-AHG, only a few studies have reported on its antitumor activity by inducing apoptosis in HCT116 human colon cancer cells [40], its skin-whitening activity by inhibiting melanin production in B16F10 murine melanoma cells [18, 39] and human epidermal melanocytes [17], and its promotion of hyaluronic acid production in human keratinocyte HaCaT cells, which is beneficial for skin hydration and repair [23]. Additionally, L-AHG has been shown to inhibit NO production in mouse macrophage RAW264.7 cells exposed to LPS [39], suggesting its potential anti-inflammatory properties by modulating the LPS-induced inflammatory response of M1 macrophages. Nevertheless, the anti-inflammatory activity of L-AHG remains largely unexplored, with the exception of a study showing its inhibitory efficacy on NO production in LPS-treated RAW264.7 cells. There is a paucity of detailed studies on the cellular biochemical mechanisms underlying this activity.

The present study aimed to elucidate the impact of L-AHG on the LPS-induced pro-inflammatory response of the RAW264.7 mouse macrophage cell line. This was done to obtain further insight into the mechanisms by which L-AHG exerts its anti-inflammatory effects on macrophages. In this context, several inflammatory responses of RAW264.7 cells that can be induced by LPS treatment, including TLR4-mediated ROS generation, MyD88-dependent activation of MAPKs (JNK and p38 MAPK) and upregulation of COX-2 expression, as well as TRIF-dependent upregulation of iNOS expression, were compared in the absence and presence of

L-AHG co-treatment.

Materials and Methods

Reagents, chemicals, antibodies, and cells

LPS (*Escherichia coli* serotype 055:B5), FITC-conjugated LPS (FITC-LPS), Griess reagent, 3-(4,5-dimenthylthiazol-2-yl)-2,5-diphenyl-tetrazolium bromide (MTT), 1,1-diphenyl-2-picryl-hydrazl (DPPH), and α-tocopherol (α-TOC) were purchased from Sigma-Aldrich (St. Louis, MO, USA). An ECL western blot kit was purchased from GE Healthcare Life Science (Little Chalfont, Buckinghamshire, UK). Neoagaro-oligosaccharide (NA2, NA4 and NA6) and L-AHG were obtained from AT-31 BIO (Daegu, Korea). The anti-GAPDH and APC conjugated anti-CD206 were purchased from Invitrogen (Carlsbad, CA, USA). The anti-COX-II, anti-JNK, and anti-p38 MAPK were obtained from Santa Cruz Biotechnology (Santa Cruz, CA). The anti-iNOS antibody was obtained from BD Biosciences (Franklin Lakes, NJ, USA). The anti-p-TAK1 (T187) was purchased from Abcam (Cambridge, UK). The anti-arginase-1 antibody was purchased from Proteintech (Rosemont, IL, USA). The RAW264.7 mouse macrophage cell line was obtained from ATCC (Manassas, VA, USA) and maintained in Dulbecco's modified Eagle's medium (DMEM) containing 10% FBS and 100 μg/ml gentamycin in a humidified 5% CO_2 incubator at 37℃. The cells were grown to 80–90% confluency for the experiments and used for up to 20 passages.

Nitric oxide assay

As a parameter of NO production, the concentration of nitrite, a stable metabolite of NO, in the culture medium was assessed by Griess reagent [12, 37]. Briefly, RAW264.7 cells (2×10^5 cells/well) were cultured overnight in 96-well plates, and then treated with 0.1 μg/ml LPS for 16 hr in the absence or presence of various concentrations of L-AHG, NA2, NA4, or NA6 for 16 hr. The culture supernatant (100 μl) was mixed with an equal volume of Griess reagent for 15 min at room temperature in dark condition, and then the absorbance of the chromophoric azo-derivative molecule was measured at 540 nm using a microplate reader. To ensure the validity of the results, experiments were done in three independent experiments with three replicates per each independent experiment.

Cell viability assay

The cell viability was measured using the MTT assay as previously described [15]. Briefly, the cells (2.5×10^5 cells/well) were incubated overnight in 96-well plates and subsequently exposed to 0.1 μg/ml LPS for 16 hr in the absence or presence of the individual compounds (L-AHG, NA2, NA4, or NA6). Subsequently, 50 μl of 1.1 mg/ml MTT solution was added to each well and incubated for additional 4 hr. The colored formazan crystals were dissolved in DMSO, and OD values of the solutions at 540 nm were measured using a microplate reader.

Preparation of cell lysate and Western blot analysis

Cell lysates were prepared by suspending cells (3×10^6) in 150 μl of lysis buffer (137 mM NaCl, 15 mM EGTA, 1 mM sodium orthovanadate, 15 mM $MgCl_2$, 25 mM MOPS, 1 mM PMSF, and 5.0 μg/ml proteinase inhibitor E-64, 0.1% Triton X-100, pH 7.2) as described elsewhere [15]. The cells were disrupted by sonication and extracted at 4℃ for 30 min. An equivalent amount of protein lysate (20 μg) was electrophoresed on 4–12% NuPAGE gradient gel (Invitrogen/Novex, Carlsbad, CA, USA) with MOPS buffer and then transferred onto Immobilon-P membranes. Detection of each protein was performed utilizing the ECL Western blotting kit following the manufacturer's instructions. The protein bands were detected using an ECL western blotting kit. Densitometry was carried out using ImageQuant TL software (Amersham, Arlington Heights, IL, USA). The arbitrary densitometric units of the protein of interest were corrected for those of GAPDH.

DPPH radical-scavenging activity assay

After 800 μl of DPPH radical solutions (0.2 mM DPPH in ethanol) were mixed with 50 μl of the agarose hydrolysates in DMSO and incubated at 37℃ for 30 min, the absorbance at 517 nm was measured. All determinations were performed in triplicate [37].

Flow cytometric analysis

To measure the intracellular ROS production, 2',7'-dichlorofluorescein diacetate (DCFH-DA) was used as a fluorescent probe as described previously [7]. After the cells (1.0×10^6) were incubated with 50 μM DCFH-DA at 37℃ for 30 min, the fluorescence intensity was analyzed by flow cytometry at an excitation wavelength of 488 nm. Flow cytometric analysis of LPS binding to TLR4 on RAW264.7 cells was performed, as described previously [13]. Briefly, 1.0×10^6 cells were pretreated with L-AHG for 1 hr and then exposed to FITC-conjugated LPS (0.1 μg/ml) at 37℃ for 30 min. The

cells were washed with cold PBS, fixed with 1% paraformaldehyde at 4℃ for 30 min, and suspended in PBS for analysis. The fluorescence intensity was analyzed by flow cytometry. A 100-fold excess of non-labeled LPS was added to confirm the specific binding.

Statistical analysis

Unless otherwise indicated, the data presented are representative of at least three independent experiments. All data are expressed as the mean ± standard deviation (for each group, n≤3). Statistical analyses were performed using the Student's *t*-test to evaluate the significance of differences between two groups, and one-way ANOVA followed by Dunnett's multiple comparison test to compare three or more groups. $p<0.05$ was considered statistically significant. The statistical analysis was conducted using SPSS Statistics version 23 (IBM, Armonk, NY, USA).

Results and Discussion

Comparison of the anti-NO production activities of agarose hydrolysates in LPS-stimulated RAW264.7 murine macrophage cell line

The RAW264.7 cell line was derived from a male BALB/c mouse and has been immortalized by Abelson murine leukemia virus transformation, resulting in a macrophage-like cell line [33, 34]. Due to their functional stability in performing both phagocytosis and pinocytosis, RAW264.7 cells have been adopted as an excellent model for investigating the functional role of macrophages in the immune system. Furthermore, RAW264.7 cells in their basal state as M0 macrophages possess the capacity to polarize into either the M1 pro-inflammatory or the M2 anti-inflammatory phenotype, providing a proper model to study the effects of various cytokines and environmental factors on macrophage polarization and immune responses [16, 28].

To compare the anti-inflammatory activities of L-AHG and neoagaro-oligosaccharides (NA2, NA4, and NA6), the individual compounds were tested for their anti-NO production activity using LPS-stimulated RAW264.7 cells. When the cells were treated with LPS in the presence of L-AHG, NA2, NA4, or NA6 at concentrations ranging from 100 to 500 μg/ml, LPS-induced production of NO was reduced in a dose-dependent manner, with L-AHG exhibiting the most significant inhibitory effect (Fig. 1A). However, the other neoagaro-oligosaccharides tested did not demonstrate any notable influence on the LPS-induced NO production. The presence of 100 μg/ml L-AHG resulted in inhibition of more than 50% of the LPS-induced NO production. In addition, the effect of 25–200 μg/ml L-AHG on LPS-induced NO production was investigated to measure the EC_{50} value of anti-NO production activity of L-AHG. As a result, the EC_{50} value of L-AHG against LPS-induced NO production in RAW264.7 cells was determined to be 135.6 μg/ml (Fig. 1B). Under the same conditions, neither L-AHG nor other neoagaro-oligosaccharides at experimental concentrations tested exhibited any effect on

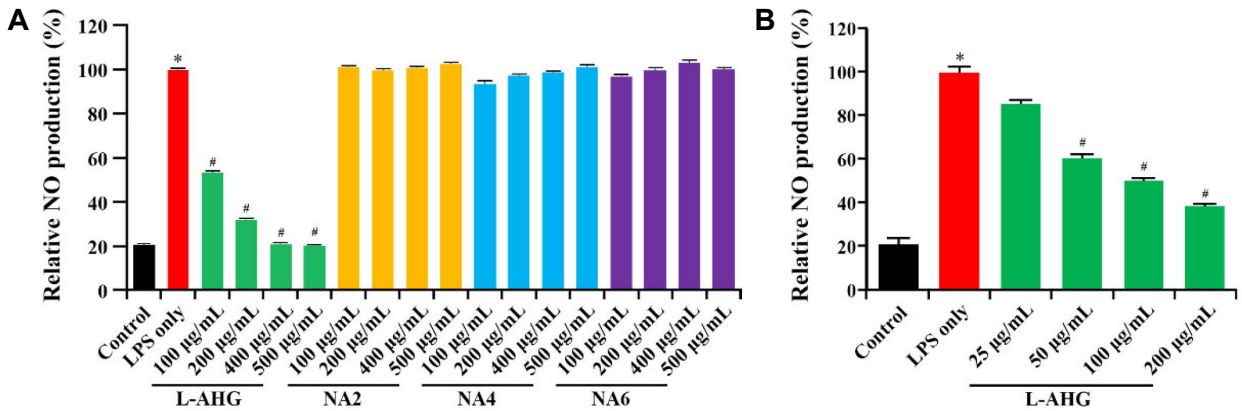

Fig. 1. Effect of L-AHG, NA2, NA4, and NA6 on the production of NO (A, B) in LPS-stimulated RAW264.7 cells. After the cells (2.5×10^5 cells/well) were incubated in 96-well plates overnight, they were preincubated with L-AHG, NA2, NA4, and NA6 (100 μg/ml, 200 μg/ml, 400 μg/ml, and 500 μg/ml for A) or only L-AHG (25 μg/ml, 50 μg/ml, 100 μg/ml, and 200 μg/ml for B) for 1 hr before incubation with LPS (0.1 μg/ml) for 16 hr. Nitrite concentration accumulation in the culture medium was measured as described in Material and Methods. Equivalent cultures were prepared and incubated for 16 hr to measure cell viability using the MTT assay. Data represent the mean ± SD of three independent experiments performed in triplicate. *$p<0.05$, significant compared with vehicle-treated control. $^{\#}p<0.05$, significant compared with LPS alone. Symbols: L-AHG, 3,6-anhydro-L-galactose; NA2, neoagarobiose; NA4, neoagaroteraose; NA6, neoagarohexaose.

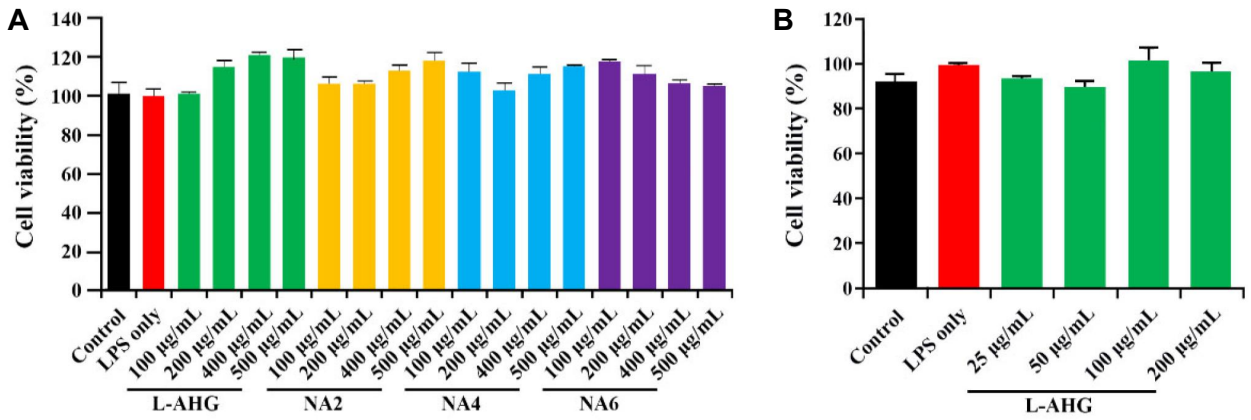

Fig. 2. Effect of L-AHG, NA2, NA4, and NA6 on the cell viability in LPS-stimulated RAW264.7 cells. After RAW264.7 cells (2×10^5 cells/well) were incubated in 96-well plates overnight, the cells were pretreated with the individual compounds for 1 hr before incubation with LPS (0.1 μg/ml) for 16 hr. The cell viability was measured using the MTT assay as described in Materials and Methods. Each value is expressed as mean ± SD (n=3 with six replicates per independent experiment). Symbols: L-AHG, 3,6-anhydro-L-galactose; NA2, neoagarobiose; NA4, neoagaroteraose; NA6, neoagarohexaose.

the viability of RAW264.7 cells (Fig. 2A). These results demonstrate that L-AHG inhibits the LPS-induced NO production with an EC50 value of 135.6 μg/ml, while maintaining the viability of RAW264.7 cells.

Effect of L-AHG on LPS-induced intracellular ROS production in RAW264.7 cells

Previous studies have reported the involvement of intracellular NADPH oxidase-mediated generation of reactive oxygen species (ROS) in the LPS-induced pro-inflammatory signaling pathway, leading to the promotion of NF-κB activation in macrophages [14, 19]. The stimulation of macrophages by LPS has been demonstrated to provoke p38 MAPK-mediated phosphorylation of p47phox, a cytosolic subunit of NADPH, which participates in the assembly of active NADPH oxidase [2, 21].

To ascertain whether the ROS generation induced by LPS in RAW264.7 cells can be influenced by L-AHG co-treatment, intracellular ROS levels in RAW264.7 cells treated with LPS alone were compared to those in RAW264.7 cells treated with LPS plus various concentrations of L-AHG (25–200 μg/ml). When the change in the intracellular ROS level of RAW264.7 cells after exposure to LPS was measured by flow cytometry using DCFH-DA staining, which detects ROS, the MFI value of the non-treated control was elevated by 1.86-fold after exposure to LPS for 22 hr (Fig. 3A). In the presence of L-AHG, the LPS-induced elevation of intracellular ROS levels in RAW264.7 cells was reduced in a dose-dependent manner.

Given that L-AHG was able to prevent the LPS-induced generation of intracellular ROS in RAW264.7 cells, we proceeded to test whether L-AHG possesses free radical-scavenging activity *in vitro* using the DPPH method. As shown in Fig. 3B, none of the L-AHG, NA2, NA4, and NA6 at a concentration of 1 mg/ml exhibited a notable level of the DPPH radical-scavenging activity *in vitro*. In contrast, 1.0 mM α-TOC scavenged DPPH radicals to a considerable extend.

Consequently, these results indicate that the inhibitory effect of L-AHG on LPS-induced ROS generation in RAW264.7 cells was due to the interference of pro-inflammatory signaling processes with ROS production, rather than due to the direct free radical-scavenging activity, which was easily detected by the antioxidant α-TOC.

Effect of L-AHG on LPS-induced activation of TAK1, JNK, and p38 MAPK and expression of iNOS and COX-II

It is well established that the LPS-induced inflammatory response of macrophages is accompanied by the production of critical pro-inflammatory mediators, including NO and prostaglandin E2 (PGE2). The production of these mediators is known to be governed by the enzymes iNOS and COX-2, respectively. To examine the mechanisms underlying the anti-NO production activity of the L-AHG, we investigated whether the L-AHG could suppress the expression levels of iNOS and COX-2 in LPS-stimulated RAW264.7 cells by western blot analyses. As shown in Fig. 4A, the iNOS and COX-II proteins were not expressed in unstimulated RAW264.7 cells. However, their levels were commonly upregulated in LPS-

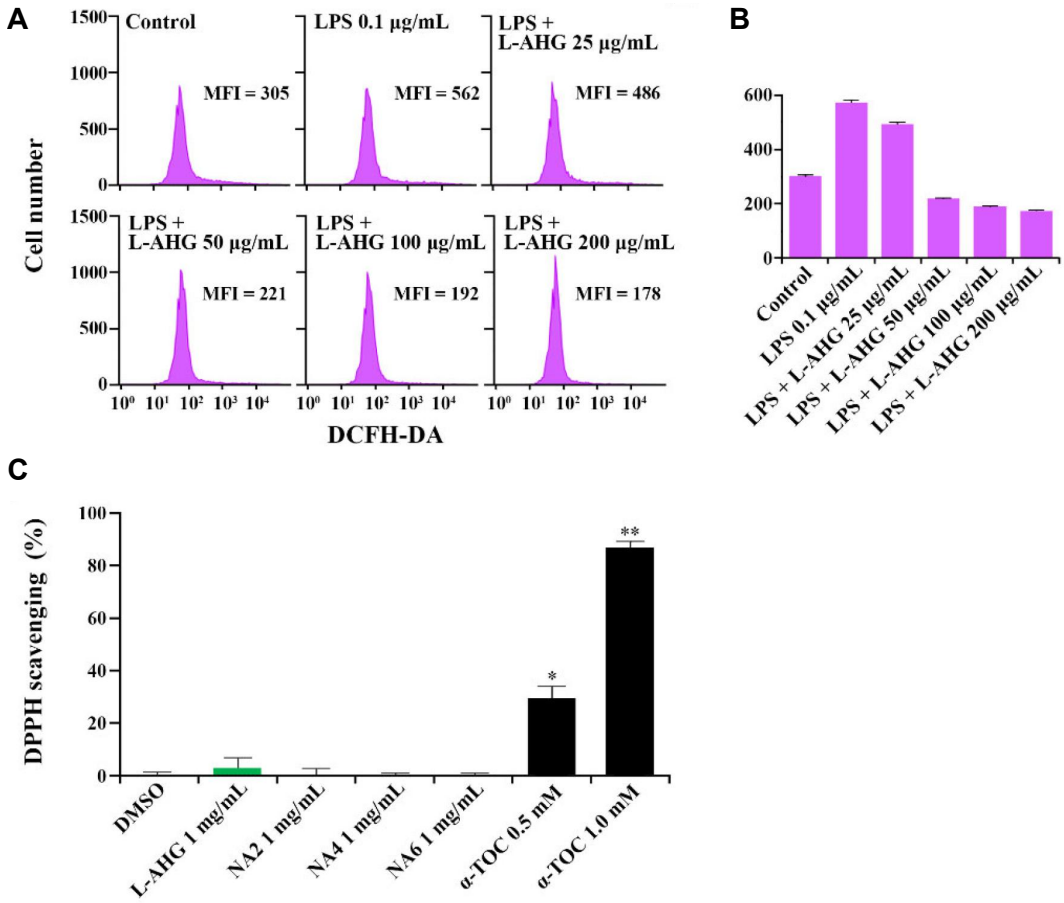

Fig. 3. Suppressive effect of L-AHG on intracellular ROS generation in LPS-activated RAW264.7 cells (A and B), and *in vitro* DPPH radica-scavenging activity of L-AHG (C). The cells were pretreated with L-AHG (25, 50, 100, or 200 μg/ml) for 1 hr and then stimulated with 0.1 μg/ml LPS for 22 hr. The cells were then harvested and subjected to detection of intracellular ROS by flow cytometry using DCFH-DA staining. The intracellular ROS level was indicated by the mean fluorescent intensity (MFI) ± SD from three separate experiments. The free radical scavenging activity of L-AHG, NA2, NA4, and NA6 at concentration of 1 mg/ml against DPPH were compared to those of a-tocopherol at concertation of 0.5 and 1.0 mM. DPPH contents in the reaction mixtures were assessed as described in Materials and methods. Data represent the mean ± SD of three independent observations performed in triplicate. *p<0.05, **p<0.01, significant compared with vehicle-treated control.

treated RAW264.7 cells for 16 hr. However, following pretreatment with 25 to 200 μg/ml of L-AHG, the LPS-induced iNOS expression levels were decreased in a dose-dependent manner. It is noteworthy that the LPS-induced up-regulation of the COX-II protein level was reduced by L-AHG, although to a lesser extent than the reduction observed in the iNOS protein level. These results demonstrate that the anti-NO production activity of L-AHG was attributable to its suppression of the up-regulation of the iNOS protein level induced in LPS-stimulated RAW264.7 cells.

To ascertain whether the protein kinases involved in TLR4-mediated MyD88-dependent proximal signaling events are targeted by the inhibitory action of L-AHG in LPS-stimulated RAW264.7 cells, the effect of L-AHG on the LPS-induced activation of TAK1, JNK, and p38 MAPK was investigated. The activation of TAK1, JNK, and p38 MAPK induced by LPS was analyzed by western blotting using antibodies specific for the phosphorylated active forms of these proteins. The activation of JNK and p38 MAPK, which is known to be dictated by the TLR4-TAK1 pathway, was confirmed through the elevation of their activating phosphorylation levels, as previously described [21, 32, 37].

As shown in Fig. 4B, the phosphorylated forms of TAK1 at Thr-187, JNK at Thr-183/Tyr-185, and p38 MAPK at Thr-180/Tyr-182 were not or barely detected in unstimulated RAW264.7 cells. However, following treatment with LPS, the activating phosphorylation of TAK1, JNK, and p38 MAPK was readily discernible, indicating that these proteins

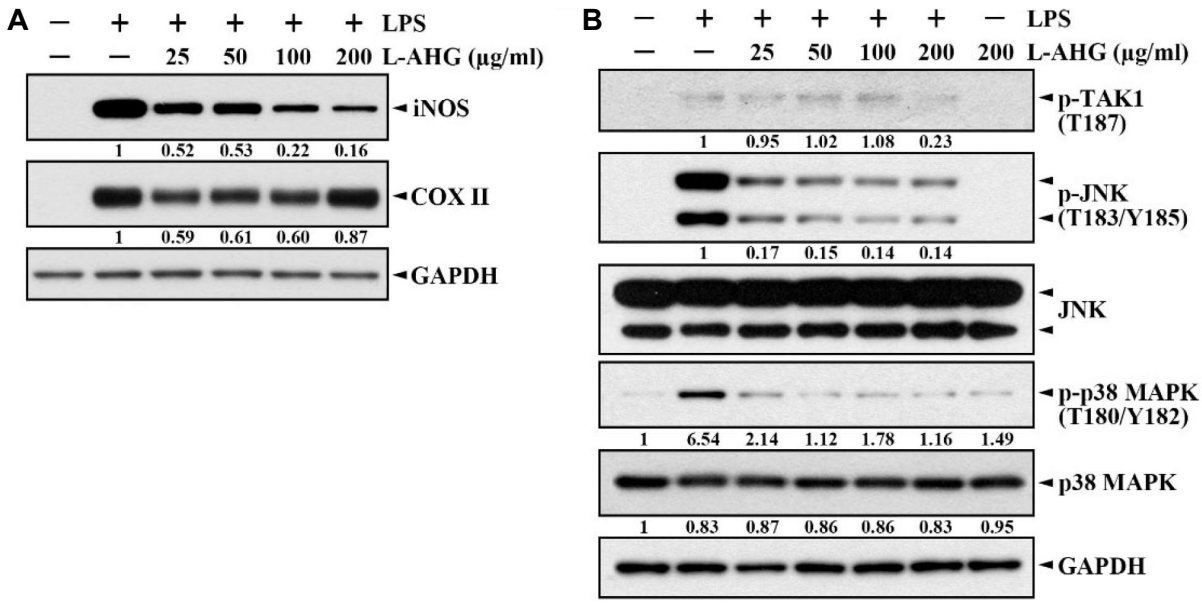

Fig. 4. Effect of L-AHG on the levels of phospho-TAK1 (T187), phosphor-JNK (T183/Y185), JNK, phosphor-p38 MAPK (T180/Y182), and p38 MAPK. The cells were pretreated with L-AHG at the incidaed concentrations for 1 hr and then stimulated with LPS (0.1 μg/ml) for 15 min (A) or 22 hr (B), respectively. After preparing the cell lysates, equivalent amounts of cell lysates (20 μg) were electrophoresed and electrotransferred onto a nylon membrane for western blot analysis as described in Materials and Methods. Representative results are shown and two additional experiments yielded similar results.

underwent conversion into active forms in RAW264.7 cells in response to LPS treatment. It is noteworthy that the LPS-induced activating phosphorylation of JNK and p38 MAPK was inhibited by L-AHG, whereas the LPS-induced activating phosphorylation of TAK1 was not influenced by L-AHG (25−100 μg/ml), with the exception of 200 μg/ml L-AHG. Given that the TLR4-mediated signaling pathway transmits the pro-inflammatory signal that is crucial for TAK1 activation and subsequent activation of IKK and MAPKs in LPS-treated macrophages, it seems likely that L-AHG may interfere with the TAK1 activity required for activating phosphorylation of JNK and p38 MAPK.

Consequently, these results suggest that the anti-NO production and anti-ROS production activities of L-AHG observed in LPS-treated RAW264.7 cells are primarily attributable to its inhibitory effect on TAK1-mediated activating phosphorylation of JNK and p38 MAPK.

Effect of L-AHG on the association between LPS and TLR4 on the surface of RAW264.7 cells

Although L-AHG exists in nature as a rare sugar comprising agarose, we sought to determine whether the inhibitory effect of L-AHG on pro-inflammatory signaling events induced in LPS-treated RAW264.7 cells is due to impaired association of LPS with the cell surface receptor TLR4 in the presence of L-AHG. When the binding of LPS to the surface of RAW264.7 cells was compared by flow cytometry following treatment with either FITC-LPS alone or FITC-LPS plus a 100-fold excess of nonlabeled LPS, the FITC-LPS binding on the cell surface was readily discernible, yet was entirely abrogated in the presence of a 100-fold excess of nonlabeled LPS (Fig. 5). In contrast, the binding of FITC-LPS on the cell surface was not affected by L-AHG at concentrations of 100–200 μg/ml. This indicates that the interaction of LPS with TLR4 is not a target of the anti-inflammatory action of L-AHG. Consequently, these findings support the conclusion that the anti-inflammatory efficacy of L-AHG is mediated by the inhibition of TAK1-mediated activating phosphorylation of JNK and p38 MAPK, which can manifest as suppression of NO and ROS production in LPS-treated RAW264.7 cells.

In summary, the anti-NO production effects of enzymatic agarose hydrolysates, including L-AHG, NA2, NA4, and NA6, were compared in the LPS-stimulated RAW264.7 mouse macrophage cell line. Consequently, only L-AHG demonstrated the capacity to suppress LPS-induced NO production and LPS-induced iNOS up-regulation, which is a well-established marker of M1 macrophage polarization. LPS-induced

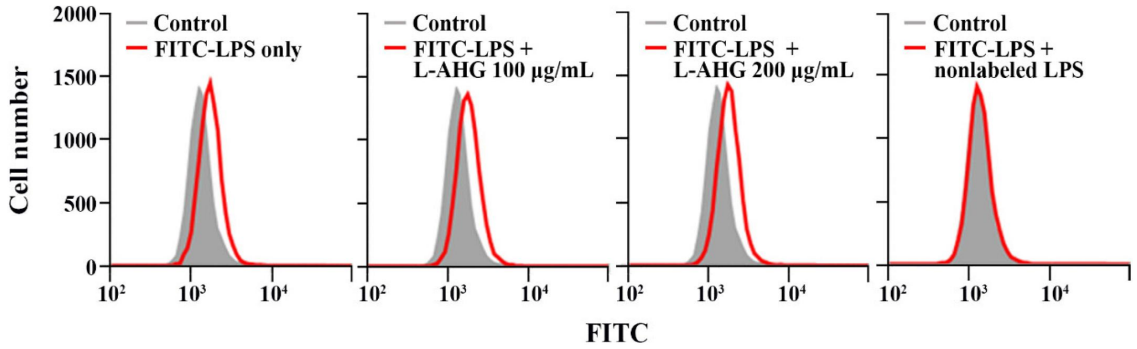

Fig. 5. Inhibitory effect of L-AHG on the binding of FITC-LPS to the surface of LPS-stimulated RAW264.7 cells. For flow cytometric analysis of FITC-LPS binding to the surface of RAW264.7 cells, the cells pretreated with L-AHG for 1 hr were then exposed to either FITC-LPS (0.1 μg/ml) or FITC-LPS (0.1 μg/ml) plus a 100-fold excess of nonlabeled LPS for 30 min. The fluorescence intensity was analyzed by flow cytometry. Representative results are shown, and two additional experiments yielded similar results.

up-regulation of cyclooxygenase-2 (COX-2), which catalyzes the generation of prostaglandin E2, an inflammatory mediator, was also reduced by L-AHG. Furthermore, the MTT assay results demonstrated that L-AHG did not exhibit cytotoxicity toward RAW264.7 cells. A dose-dependent reduction in LPS-induced intracellular ROS generation by L-AHG was observed at concentrations ranging from 25 to 200 μg/ml. However, L-AHG at a concentration of up to 1 mg/ml failed to exhibit a remarkable DPPH radical-scavenging activity *in vitro*. These results suggest that L-AHG may be capable of blocking the TLR4-mediated pro-inflammatory signaling pathway, which generates intracellular ROS in LPS-stimulated RAW264.7 cells. With regard to the pro-inflammatory signaling process targeted by L- AHG, it was observed that it did not affect TLR4-TAK1 activation pathway, representing the proximal pro-inflammatory signal transduction cascade induced in LPS-treated RAW264.7 cells. However, L-AHG was found to reduce the activating phosphorylation of JNK and p38 MAPK, both of which are known to be driven by TAK1 during the LPS-induced TLR4-mediated pro-inflammatory signaling pathway. Conversely, the specific interaction between LPS and its receptor TLR4 on the surface of RAW264.7 cells does not appear to be the target of the anti-inflammatory action of L- AHG. This evidence supports the notion that the anti-inflammatory action of L-AHG targets the LPS-induced TLR4-mediated proximal pro-inflammatory signaling process, including the TAK-dependent JNK/p38 MAPK activation phase. TAK1 plays a pivotal role in the pro-inflammatory signaling pathway in LPS-stimulated macrophages, as it is involved in the activation of transcription factor NF-κB, JNK, and p38 MAPK through catalyzing their activating phosphorylation [9, 24, 30]. The active p38 MAPK then contributes to the assembly of active NADPH, leading to the intracellular generation of pro-inflammatory ROS [19, 21]. Consequently, these findings indicate that the L-AHG-mediated prevention of the TAK1-JNK/p38 MAPK activation step of the pro-inflammatory signal transduction process in LPS-stimulated macrophages by L-AHG represents a valuable mechanism to inhibit M1 polarization and pro-inflammatory responses in macrophages.

Acknowledgement

This work was supported by the Technology Development Program (RS-2023-00257262) funded by the Ministry of SMEs and Startups (MSS, Korea).

The Conflict of Interest Statement

The authors declare that they have no conflicts of interest with the contents of this article.

References

1. Beaumont, M., Tran, R., Vera, G., Niedrist, A., Rousset, A., Pierre, R., Shastri, V. P. and Forget, A. 2021. Hydrogel-forming algae polysaccharides: From seaweed to biomedical applications. *Biomacromolecules* **22**, 1027-1052.
2. Bokoc, G. M. and Knaus, U. G. 2003. NADPH oxidases: not just for leukocytes anymore. *Trends. Biochem. Sci.* **28**, 502-508.
3. Chaintreuil, P., Kerreneur, E., Bourgoin, M., Savy, C., Favreau, C., Robert, G., Jacquel, A. and Auberger, P. 2023. The generation, activation, and polarization of monocyte-derived macrophages in human malignancies. *Front. Immunol.* **14**, 1178337.
4. Charles, D. M. and Klaus, L. 2014. M1 and M2 macro-

phages: the chicken and the egg of immunity. *J. Innate. Immun*. **6,** 716-726.
5. Chen, S., Saeed, A. F. U. H., Liu, Q., Jiang, Q., Xu, H., Xiao, G. G., Rao, L. and Duo, Y. 2023. Macrophages in immunoregulation and therapeutics. *Signal Transduct. Target. Ther.* **8**, 207.
6. Corriveau, C. C. and Danner, R. L. 1993. Endotoxin as a therapeutic target in septic shock. *Infect. Agents Dis.* **2**, 35-43.
7. Diakalov, S., Griendling, K. K. and Harrison, D. G. 2007. Measurement of reactive oxygen species in cardiovascular studies. *Hypertension* **49**, 717-727.
8. Duckworth, M. and Yaphe, W. 1971. The structure of agar. Part I. Fractionation of a complex mixture of polysaccharides. *Carbohydr. Res.* **16**, 189-197.
9. Fujihara, M., Muroi, M., Tanamoto, K., Suzuki, T., Azuma, H. and Ikeda, H. 2003. Molecular mechanisms of macrophage activation and deactivation by lipopolysaccharide: roles of the receptor complex. *Pharmacol. Ther.* **100**, 171-194.
10. Gao, J. J., Filla, M. B., Fultz, M. J., Vogel, S. N., Russell, S. W. and Murphy, W. J. 1998. Autocrine/paracrine IFN-α β mediates the lipopolysaccharide-induced activation of transcription factor Stat1α in mouse macrophages: pivotal role of Stat1α in induction of the inducible nitric oxide synthase gene. *J. Immunol.* **161**, 4803-4810.
11. Gharavi, A. T., Hanjani, N. A., Movahed, E. and Doroudian, M. 2022. The role of macrophage subtypes and exosomes in immunomodulation. *Cell. Mol. Biol. Lett.* **27**, 83.
12. Green, L. C., Wanger, D. A. and Glogowski, J. 1982. Analysis of nitrate, nitrite, and [^{15}N] nitrate in biological fluids. *Anal. Biochem.* **126**, 131-138.
13. Hussain, S. F., Yang, D., Suki, D., Aldape. K., Grimm. E. and Heimberger. A. B. 2006. The role of human glioma-infiltrating microglia/macrophages in mediating antitumor immune responses. *Neuro. Oncol*. **8**, 261-279.
14. Janessen-Heininger, Y. M., Poynter, M. E. and Baeuerle, P. A. 2000. Recent advances towards understanding redox mechanisms in the activation of nuclear factor κB. *Free Radic. Biol. Med.* **28**, 1317-1327.
15. Jun, D. Y., Kim, J. S., Park, H. S., Han, C. R., Fang, Z., Woo, M. H., Rhee, I. K. and Kim, Y. H. 2007. Apoptogenic activity of *Zanthoxylum schinifolim* toward human acute leukemia Jurkat T cells is associated with ER stress-mediated caspase-8 activation that stimulates mitochondria-dependent or -independent caspase cascade. *Carcionogenesis* **28**, 1303-1313.
16. Khabipov, A., Kading, A., Liedtke, K. R., Freund, E., Partecke, L. I. and Bekeschus, S. 2019. RAW264.7 macrophage polarization by pancreatic cancer cells - a model for studying tumour-promoting macrophages. *Anticancer Res.* **39**, 2871-2882.
17. Kim, J. H., Kim, D. H., Cho, K. M., Kim, K. H. and Kang, N. J. 2018. Effect of 3,6-anhydro-l-galactose on α-melanocyte stimulating hormone-induced melanogenesis in human melanocytes and a skin-equivalent model. *J. Cell. Biochem.* **119**, 7643-7656.
18. Kim, J. H., Yun, E. J., Yu, S., Kim, K. H. and Kang, N. J. 2017. Different levels of skin whitening activity among 3,6-anhydro-L-galactose, agaro-oligosaccharides, and neoagaro-oligosaccharides. *Mar. Drugs* **15**, 321.
19. Kong, X., Thimmulappa, R., Kombairaju, P. and Biswal, S. 2010. NADPH oxidase-dependent reactive oxygen species mediate amplified TLR4 signaling and sepsis-induced mortality in Nrf2-deficient mice. *J. Immunol.* **185**, 569-577.
20. Kubes, P. and McCafferty, D. M. 2000. Nitric oxide and intestinal inflammation. *Am. J. Med.* **109**, 150-158.
21. Laroux, F. S., Romero, X., Wetzler, L., Engel, P. and Terhorst, C. 2005. Cutting edge: MyD88 Controls phagocyte NADPH oxidase function and killing of gram-negative bacteria. *J. Immunol.* **175**, 5596-5600.
22. Lee, H., Fessler, M. B., Qu, P., Heymann, J. and Kopp, J. B. 2020. Macrophage polarization in innate immune responses contributing to pathogenesis of chronic kidney disease. *BMC Nephrol.* **21**, 270.
23. Lee, J. E., Kim, Y. A., Yu, S., Park, S. Y., Kim, K. H. and Kang, N. J. 2019. 3,6-Anhydro-L-galactose increases hyaluronic acid production via the EGFR and AMPKα signaling pathway in HaCaT keratinocytes. *J. Dermatol. Sci.* **96**, 90-98.
24. Lu, Y. C., Yeh, W. C. and Ohashi, P. S. 2008. LPS/TLR4 signal transduction pathway. *Cytokine* **42**, 145-151.
25. Luo, M., Zhao, F., Cheng, H., Su, M. and Wang, Y. 2024. Macrophage polarization: an important role in inflammatory diseases. *Front. Immunol.* **15**, 1352946.
26. Miao, X., Leng, X. and Zhang, Q. 2017. The current state of nanoparticle-induced macrophage polarization and reprogramming research. *Int. J. Mol. Sci.* **18**, 336.
27. Murray, P. J. 2017 Macrophage polarization. *Annu. Rev. Physiol.* **10**, 541-566.
28. Orekhov, A. N., Orekhova, V. A., Nikiforov, N. G., Myasoedova, V. A., Grechko, A. V., Romanenko, E. B., Zhang, D. and Chistiakov, D. A. 2019. Monocyte differentiation and macrophage polarization. *Vessel Plus.* **3**, 10.
29. Raggi, F., Pelassa, S., Pierobon, D., Penco, F., Gattorno, M., Novelli, F., Eva, A., Varesio, L., Giovarelli, M. and Bosco, M. C. 2017. Regulation of human macrophage M1-M2 polarization balance by hypoxia and the triggering receptor expressed on myeloid cells-1. *Front. Immunol.* **8**, 1097.
30. Rhee, S. H. and Hwang, D. 2000. Murine TOLL-like receptor 4 confers lipopolysaccharide responsiveness as determined by activation of NFκB and expression of the inducible cyclooxygenase. *J. Biol. Chem.* **275**, 34035-34040.
31. Shin, K., Kararu, R. P., Park. H. J., Kwon, B. I., Kim, T. W., Hong, W. K. and Lee, S. H. 2015. T_H2 cells and their cytokines regulate formation and function of lymphatic vessels. *Nat. Commun.* **6**, 6196.
32. Shirakabe, K., Yamaguchi, K., Shibuya, H., Irie, K., Matsuda, S., Moriguchi, T., Gotoh, Y., Matsumoto, K. and Nishida, E. 1997. TAK1 mediates the ceramide signaling to stress-activated protein kinase/c-Jun N-terminal kinase.

J. Biol. Chem. **272**, 8141-8144.
33. Taciak, B., Białasek, M., Braniewska, A., Sas, Z., Sawicka, P., Kiraga, Ł., Rygiel, T. and Krol, M. 2018. Evaluation of phenotypic and functional stability of RAW264.7 cell line through serial passages. *PLoS One* **13**, e0198943.
34. Wang, S., Xiao, L., Prasadam, I., Crawford, R., Zhou, Y. and Xiao, Y. 2022. Inflammatory macrophages interrupt osteocyte maturation and mineralization via regulating the Notch signaling pathway. *Mol. Med.* **28**, 102.
35. Watson, W. H., Zhao, Y. and Chawla, R. K. 1999. S-adenosylmethionine attenuates the lipopolysaccharide-induced expression of the gene for tumor necrosis factor alpha. *Biochem. J.* **342**, 21-25.
36. Weisser, S. B., McLarren, K. W., Kuroda, E. and Sly, L. M. 2013. Generation and characterization of murine alternatively activated macrophages. *Methods Mol. Biol.* **946**, 225-239.
37. Woo, H. J., Jun, D. Y., Lee, J. Y., Park, H. S., Woo, M. H., Park, S. J., Kim, S. C., Yang, C. H. and Kim, Y. H. 2017. Anti-inflammatory action of 2-carbomethoxy-2,3-epoxy-3-prenyl-1,4-naphthoquinone (CMEP-NQ) suppresses both the MyD88-dependent and TRIF-dependent pathways of TLR4 signaling in LPS-stimulated RAW264.7 cells. *J. Ethnopharmacol.* **205**, 103-115.
38. Yuan, Z., Jiang, D., Yang, M., Tao, J., Hu, X., Yang, X. and Zeng, Y. 2024. Emerging roles of macrophage polarization in osteoarthritis: mechanisms and therapeutic strategies. *Orthop. Surg.* **16**, 532-550.
39. Yun, E. J., Lee, S., Kim, J. H., Kim, B. B., Kim, H. T., Lee, S. H., Pelton, J. G., Kang, N. J., Choi, I. G. and Kim, K. H. 2013. Enzymatic production of 3,6-anhydro-L-galactose from agarose and its purification and *in vitro* skin whitening and anti-inflammatory activities. *Appl. Microbiol. Biotechnol.* **97**, 2961-2970.
40. Yun, E. J., Yu, S., Kim, Y. A., Liu, J. J., Kang, N. J., Jin, Y. S. and Kim, K. H. 2012. *In vitro* prebiotic and anti-colon cancer activities of agar-derived sugars from red seaweeds. *Mar. Drugs* **19**, 213.

초록 : LPS에 의해 자극된 RAW264.7 대식세포에서 L-AHG에 의한 M1 분극화 및 친염증 신호경로의 억제

장원영[1] · 박신영[1,2] · 김기윤[1,2] · 전도연[2] · 배영석[1,2] · 김영호[1,2]*
([1]경북대학교 자연과학대학 생명과학부, [2]㈜에이티삼일바이오)

아가로오스의 효소가수분해산물로 부터 확보할 수 있는 3,6-무수갈락토오스(L-AHG), 네오아가로비오스(NA2), 네오아가로테트라오스(NA4) 및 네오아가로헥사오즈(NA6)의 항염증 활성을 규명하고자, 마우스 대식세포주 RAW264.7 세포를 대장균 유래 지질다당류(LPS)로 자극할 때 세포표면의 TLR4 수용체의 역할을 통해 유도되는 친염증성 M1 분극화 및 이에 따른 친염증성 반응에 미치는 영향을 조사하였다. 그 결과로서, 이들 아가로오스 분해산물들 중에서 단당류인 L-AHG만이 유일하게, LPS 자극에 의해 RAW264.7 세포에서 유도될 수 있는 M1 분극화의 대표적인 마커인 iNOS 효소의 발현과 이에 따른 NO 생성을 농도의존적으로 현저하게 저해하였고 염증 매개체인 프로스타글란딘 E2의 생성을 촉매하는 COX-2의 발현 수준도 LPS 자극후에는 증가하였지만, L-AHG의 존재에 의해서는 그 증가 수치가 다소 저해되는 것으로 나타났다. 이때 RAW264.7 세포에 대한 L-AHG의 세포독성은 확인되지 않았다. 또한 L-AHG는 LPS로 처리된 RAW264.7 세포내에서 유도되는 친염증 신호전달경로에 있어서 초기 신호전달 단계인 TAK1 활성화 단계까지는 별 영향을 나타내지 않았으나 TAK1의 촉매작용에 의한 JNK 및 p38 MAPK의 활성화 인산화(activating phosphorylation)는 현저하게 저해되었다. 특히, 대식세포의 친염증 신호전달경로에서 TAK1 활성화는, 그 하류 단계에서 NF-kB의 활성화가 성공적으로 일어날 수 있도록 해주며, 또한 TAK1에 의한 하류 신호분자인 p38 MAPK 활성화는 NADPH 활성화 및 이에 따른 친염증성 ROS 분자들의 생성을 유발하기 때문에, LPS에 의해 자극된 대식세포내의 친염증 신호전달경로에 있어서 TAK1-JNK/p38 MAPK 경로의 L-AHG에 의한 저해는 대식세포의 M1 분극화 및 친염증 반응을 억제하는 효과적인 기전이 되며, 그 활용성이 크게 기대된다. 아울러 L-AHG가 LPS와 RAW264.7 세포의 표면분자인 TLR4와 상호작용을 방해할 수 있는지에 대해서도 유세포분석기와 형광표지가 된 FITC-LPS를 이용하여 조사한 결과, L-AHG는 대식세포의 표면에서 이루어지는 LPS-TLR4 상호결합은 방해하지 않는 것으로 확인되었다. 이는 L-AHG의 항염증 작용의 표적이 LPS가 TLR4 수용체를 통해 유도하는 세포 내 신호전달경로에 있음을 지지해 준다. 이상의 연구결과들은 아가로오스 유래 희귀 단당류인 3,6-무수갈락토오스(L-AHG)가 LPS 자극에 의해 유발되는 RAW264.7 마우스 대식세포의 M1 분극화 및 염증 반응에 대해, TLR4의 친염증 신호전달경로의 TAK1-JNK/p38 MAPK 단계를 저해하는 항염증 활성을 효과적으로 발휘할 수 있음을 시사한다.